Electronic Supplementary Information

Enhanced photocatalytic activity and structural stability by hybridizing Ag_3PO_4 nanospheres with graphene oxide sheets

Qinghua Liang, Yao Shi, Wangjing Ma, Zhi Li* and Xinmin Yang*

Technical Institute of Physics and Chemistry, Chinese Academy of Sciences (CAS),
29 zhongguancun East Road, Beijing, 100190, PR China
Email: xmyang@mail.ipc.ac.cn, lizhi@mail.ipc.ac.cn

1 Experimental

1.1 Materials

Flake graphite was purchased from Sigma-Aldrich. Potassium permanganate ($KMnO_4$), potassium nitrate (KNO_3), silver nitrate ($AgNO_3$), disodium hydrogen phosphate (Na_2HPO_4), 98% sulfuric acid (H_2SO_4) solution, 30% hydrogen peroxide (H_2O_2) solution and 36–38% hydrogen chloride (HCl) were sourced from Beijing Chemical Corporation. All the reagents were used as received without further purification. Deionized (DI) water was used in all experiments.

1.2 Preparation of graphene oxide (GO)

GO sheets were prepared from natural graphite powder using a modified Hummers method.[1] In a typical procedure, 0.2 g KNO_3 and 25.0 mL 98% H_2SO_4 were placed in a beaker (250 mL) with a stirrer chip. Then 1.0 g graphite powder was slowly added under vigorous stirring. After magnetically stirring the suspension in an ice-water bath environment for about 1 h, 3.0 g $KMnO_4$ was gradually added at a temperature no

more than 5 ℃. The mixture was stirred 2 hours under low temperature conditions following by gradually heating to about 35 ℃. Afterwards, 50 mL water was slowly added into the paste over the course of about 1 h with stirring, and the temperature was kept at 90–95 ℃. The resultant suspension was further stirred for 2 h at this temperature for 30 min and then further treated with an amount of 12 mL of 30% H_2O_2 to obtain a bright yellow suspension. This suspension was continuously washed thoroughly with 3% dilute HCl and deionized water for six times. Finally, yellow-brownish sediment was obtained by centrifuging the suspension for 1 h at 8000 rpm. The obtained GO precipitate was dried at 40 ℃ under vacuum for 48 h.

1.3 Preparation of GO/Ag_3PO_4 nanocomposites

The fabrication of the GO/Ag_3PO_4 nanocomposites was undertaken by a one-step ion-exchange method approach in dark environment. Firstly, 20 mg GO was suspended in 40.0 mL deionized water with ultrasonic treatment for 2 h. A yellow stock GO dispersion was obtained after centrifuging at 5000 rpm for 30 min to remove the heavy substances and water-soluble byproduct. The mass concentration of the obtained aqueous GO dispersion was estimated to be about 0.3 mg/mL. Then 1.0 mmol $AgNO_3$ was added into above GO aqueous solution under magnetic stirring. After the mixture was stirred vigorously for 30 min, 0.03 M NaH_2PO_4 aqueous solution was dropwise added into above mixture and the resulting solution was stirred vigorously for another 60 min. During this reaction, the color of the mixture was gradually changed from bright yellow to brown. Finally, the nanocomposite powders was centrifuged and washed thoroughly with water and ethanol for several times, and then dried in dark at room temperature. For comparison, pure Ag_3PO_4 naonospheres with yellow color were also fabricated according to a similar experimental procedure, but without the addition of GO sheets.[2]

1.4 Material characterization

The phase and crystal structures of the products were identified by powder X-ray

diffraction (XRD) collected on a Bruker D8–Focus Advance X-ray diffractometer with Cu–Kα radiation (λ = 1.54056 Å) in the 2θ range from 5° to 80°. The sample was prepared by depositing sample onto a glass slide by repeated drop drying. Scanning electron spectroscopy (SEM) and energy dispersive X-ray spectroscopy (EDS) were acquired with a Hitachi S-4300 field emission scanning electron microscope. Transmission Electron Microscopy (TEM) and selected area electron diffraction (SAED) were obtained with a JEM 2100 electron microscope operating with acceleration voltage of 200 kV. Two droplet of the sample dispersed in ethanol was deposited onto a holey carbon grid and left to dry overnight at room temperature. The ultraviolet–visible–near infrared (UV-Vis-NIR) diffuse reflectance spectra (DRS) were recorded in the range from 200 to 2500 nm with a Varian Cary 5000 spectrophotometer using an integrating sphere detector. Pure $BaSO_4$ was used for background signal. Band gap energies were estimated by analysis of the Tauc's plots. Fourier transform infrared spectra (FTIR) were carried out on an Excalibur 3100 infrared spectrophotometer using KBr pellets as dispersant in the frequency range 500–4000 cm^{-1}. Raman spectra (Raman) were characterized by using a Via-Reflex Raman microprobe by employing laser of 514 nm as incident light. The photoluminescence (PL) spectra were performed on a Varian Carry Eclips 500 fluorescence spectrophotometer equipped with a 120 W xenon lamp as the excitation source. The photoactivity and the UV–visible spectra were measured on a UV–2500PC spectrophotometer. X-ray photoelectron spectroscopy (XPS) analysis was carried on an ESCALab220i-XL electron spectrometer from VG Scientific employing 300 W Al Kα as the X-ray source (1486.6 eV) at 150 W. The XPS data were fitted by the Peakfit v4.12 software and further plotted by origin 8.0. All measurements were performed at room temperature.

1.5 Photocatalytic Property Test

The photocatalytic activities of the obtained samples were evaluated by measuring the photodegradation of Rhodamine B (RhB) in aqueous solution under visible light

irradiation. In a typical measurement, a total of 35 mg photocatalysts was suspended into 100 mL of 8.0 mg/L RhB aqueous solution in a Pyrex reactor at room temperature. Prior to irradiation, the mixtures were sonicated for 15 min and then continuously magnetically stirred in the dark for 8 h to achieve the establishment of an adsorption–desorption equilibrium between RhB and the catalysts. Then the suspension was illuminated by visible light from a 500W Xe lamp equipped with cutoff filter ($\lambda > 420$ nm). At different time intervals, 2 ml solution were sampled for analysis from the reaction suspension and centrifuged to remove the photocatalyst particles. The concentration of RhB during the degradation was measured by colorimetry using a UV-vis spectrometer (Shimadzu UV-3600). The peak absorbance of RhB at 554 nm was used to determine its concentration. To assess the stability of the hybrid photocatalyst, the photocatalytic reaction was reused six times to degrade RhB under the same visible light.

2. Figures and tables

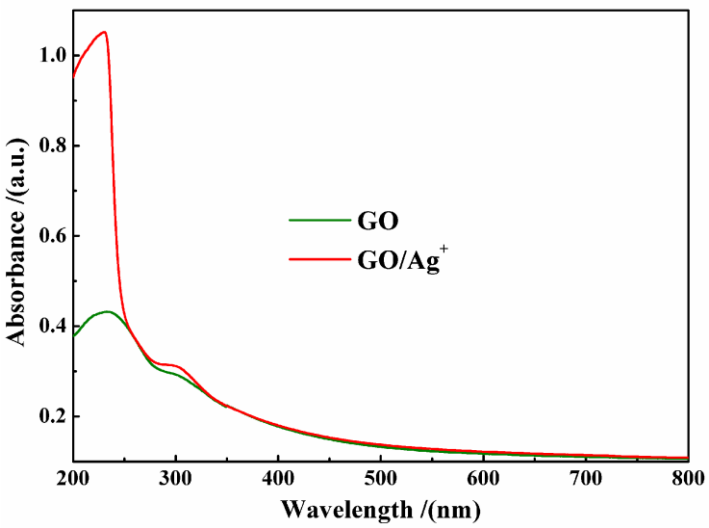

Fig. S1 UV-Vis spectra measured in aqueous solutions of GO and GO/Ag^+ for an equal concentration**.**

Two samples have a similar spectrum with a maximum absorption (λ_{max}) at around 225-231 nm and a shoulder peak around ~300 nm, which are ascribed to the

transitions of $\pi \rightarrow \pi^*$ and $n \rightarrow \pi^*$ of GO sheets, respectively.[3] However, GO/Ag^+ possesses a much higher λ_{max} than that of pure GO, which suggests that more aromatic rings or isolated aromatic domains in GO retained after adding a small amount of Ag^+.[4] The reason for this phenomenon is that the layer-stacking regularity of GO sheets would be disrupted for the intercalation of Ag^+ since the positive charged Ag^+ ions can easily anchored onto the surface of negative charged GO sheets due to the electric interaction between Ag^+ and the plenty of functional groups (hydroxyl, epoxide and carboxylic groups) of GO sheets in the aqueous solution. Thus, carbon rings in the basal planes of GO sheets was greatly maintained.

Table S1 Refined structural parameters and results for pure Ag_3PO_4 and the Ag_3PO_4 in the GO/Ag_3PO_4 nanocomposites. Fullprof program was used for the Rietveld refinements. The initial structural model was built with crystallographic data of Ag_3PO_4 (ISCD No. 201362). Wyckoff positions: Ag (0.2347, 0, 0.5), P (0, 0, 0), O (0.1484, 0.1484, 0.1484). The pseudo-Voigt function was applied for approximation of the experimental XRD patterns. The parameters including zero shifts, scale factors, background, lattices, line patterns, atom positions and site occupations were repeatedly refined in proper order. The following *Biso* and *Occ* are the abbreviations of isotropic temperature factor and occupation factor, respectively.

Parameters	Ag_3PO_4	GO/Ag_3PO_4
space group	P-43n	P-43n
a/(Å)	6.0075(3)	6.0136(8)
a/(deg)	90	90
V/(Å^3)	216.814(8)	217.481(16)
Biso(Ag)	0.03082	0.23134
Biso(P)	0.08557	0.10493
Biso(O)	0.52001	0.23294
Occ (Ag)	0.4412	0.4935
Occ (O)	0.5361	0.4380
Rf (%)	3.65	3.03
Rp (%)	5.68	6.43
Rwp (%)	7.38	8.15
Rexp (%)	7.04	7.51
Rbragg (%)	3.13	3.42

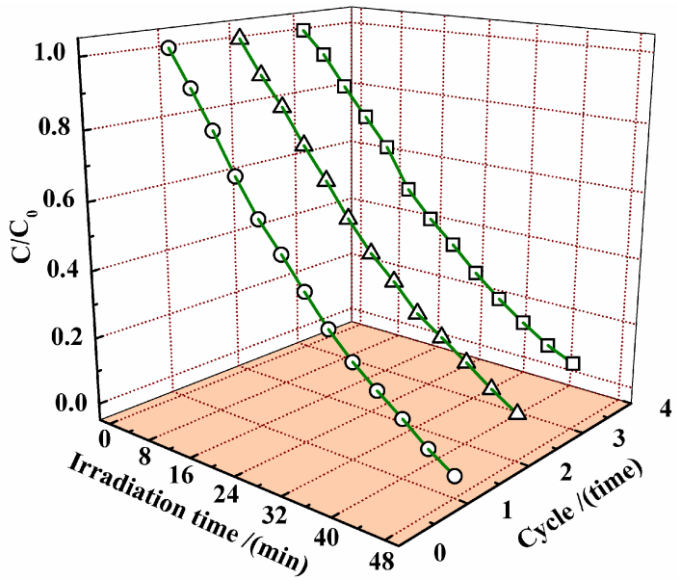

Fig. S2 Three consecutive cycles of degradation of RhB using the pure Ag_3PO_4 nanosphere as the photocatalyst.

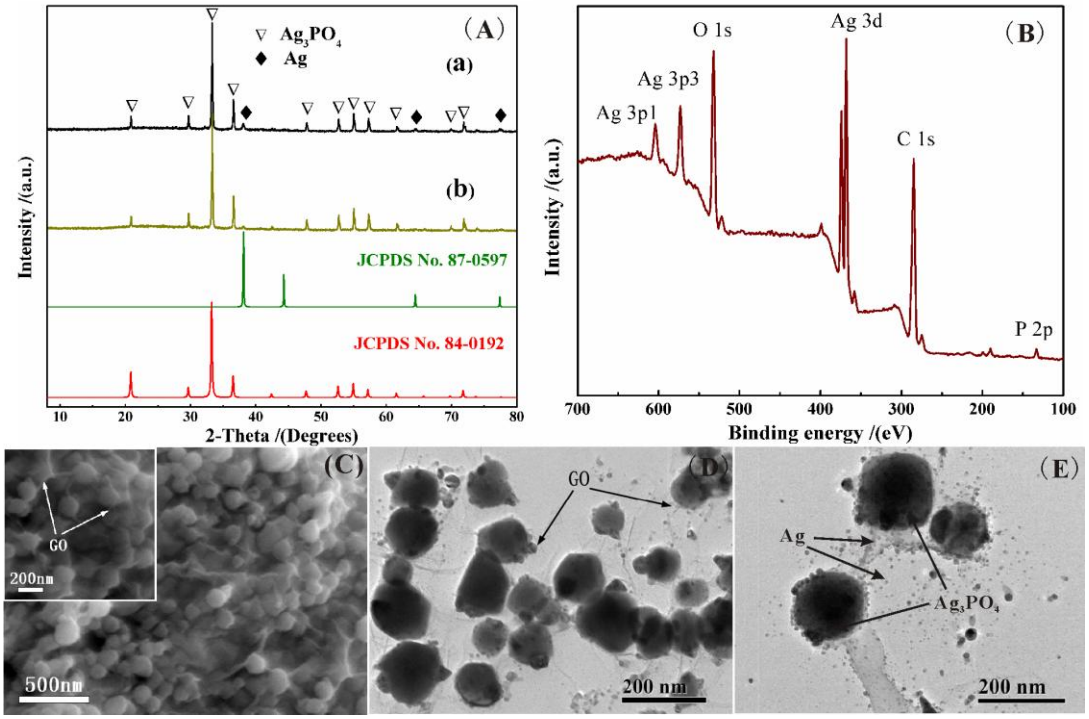

Fig. S3 (A) XRD patterns for (a) pure Ag_3PO_4 nanospheres and (b) the GO/Ag_3PO_4 nanocomposites after two and six cycle of RhB decomposition experiments, respectively; the simulated powder XRD patterns from single data are listed as reference (JCPDS No. 84-0192 and No. 87-0597). (B) XPS survey spectrum, (C) low and high-magnified SEM, and (D) TEM images obtained for the GO/Ag_3PO_4 nanocomposites after six consecutive cycles of degradation. (E) TEM image of pure Ag_3PO_4 after three consecutive cycles of degradation.

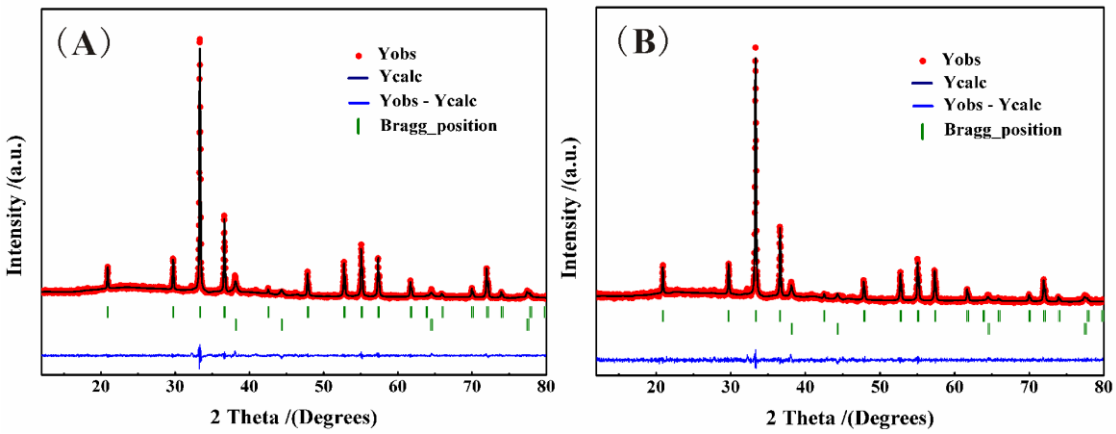

Fig. S4 Rietveld refined patterns of the as-prepared (A) pure Ag_3PO_4 nanospheres and (B) the GO/Ag_3PO_4 nanocomposites after three and six cycle of RhB decomposition experiments, respectively. The experimental data have been displayed by red dotted pattern while the black solid curve corresponds to the Rietveld fit. The green short vertical bars illustrate the Bragg reflections of the calculated pattern (Ag_3PO_4 is in the above position and Ag is in down position). The differences between the observed and calculated intensities have also been plotted in the blue curves.

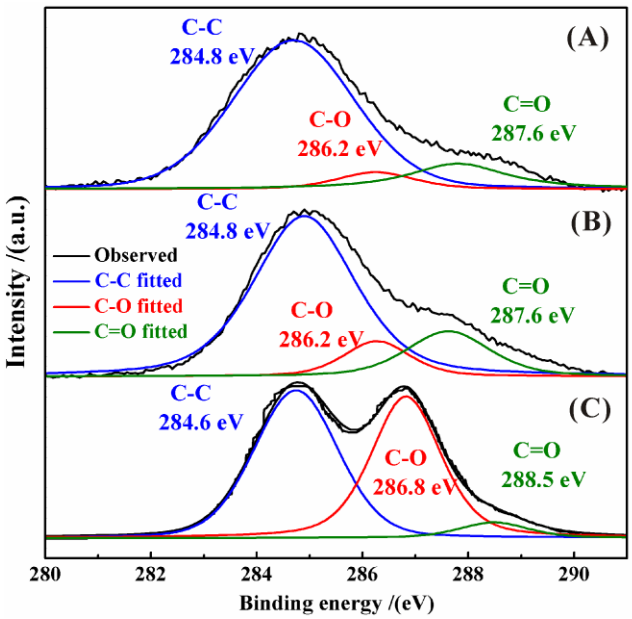

Fig. S5 C 1s XPS spectrum of GO sheets (A) and Ag_3PO_4/GO nanocomposites before (B) and after (C) the photocatalytic performance.

Typical peaks of C1s are observed in the XPS spectra of GO and the Ag_3PO_4/GO nanocomposites. The C1s peaks can be divided into three different peaks. In particular, the peak at 284.6 eV is attributed to C-C in aromatic rings, and those of at 286.8 eV and 288.5 eV are ascribed to C-O (epoxy and alkoxy) and C=O (carbonyl), respectively. [5] However, after hybridizing with Ag_3PO_4 nanospheres the peaks

corresponding to C-O and C=O of C1s moved to 286.2 eV and 287.6 eV, respectively, suggesting the strong interaction between GO sheets and the Ag_3PO_4/GO nanocomposites. Furthermore, it can be seen that the strong electron interaction still existed after photocatalytic reactions, as shown in Fig.S5 (C). Careful observation revealed that the intensity of the peaks associated with the C-O and C=O became weaker after degradation reactions. It can be concluded that little GO sheets were reduced by the photo-generated carriers.

Table S2 Refined results for pure Ag_3PO_4 nanospheres and the GO/Ag_3PO_4 nanocomposites after three and six cycle of RhB decomposition experiments, respectively. Fullprof program was used for the Rietveld refinements. The initial structural model was built with crystallographic data of Ag_3PO_4 and Ag single-crystals (ISCD No. 201362 for Ag_3PO_4 and ISCD No. 64706 for Ag). The pseudo-Voigt function was applied for approximation of the experimental XRD patterns. The parameters including zero shifts, scale factors, background, lattices, line patterns, atom positions and site occupations were repeatedly adjusted and refined in proper order.

Parameters	Ag_3PO_4	GO/Ag_3PO_4
Rp (%)	5.49	6.08
Rwp (%)	7.01	8.03
Rexp (%)	6.24	7.51
Ag (wt%)	15.6	8.8
Ag_3PO_4 (wt%)	84.4	91.2

3. References

1 W. S. Hummers and R. E. Offeman, *J. Am. Chem. Soc.*, 1958, **80**, 1339-1339.

2 A. Khan, M. Qamar and M. Muneer, *Chem. Phys. Lett.*, 2012, **519–520**, 54-58.

3 G. I. Titelman, V. Gelman, S. Bron, R. L. Khalfin, Y. Cohen and H. Bianco-Peled, *Carbon*, 2005, **43**, 641-649.

4 D. C. Marcano, D. V. Kosynkin, J. M. Berlin, A. Sinitskii, Z. Z. Sun, A. Slesarev, L. B. Alemany, W. Lu and J. M. Tour, *Acs Nano*, 2010, **4**, 4806-4814.

5 G. X. Zhao, X. M. Ren, X. Gao, X. L. Tan, J. X. Li, C. L. Chen, Y. Y. Huang and X. K. Wang, *Dalton Trans.* , 2011, **40**, 10945.